Velocity selection in a Doppler-broadened ensemble of atoms interacting with a monochromatic laser beam

Ifan G. Hughes[a]

[a]Joint Quantum Centre (JQC) Durham-Newcastle, Department of Physics, Durham University, Durham DH1 3LE, UK

ARTICLE HISTORY
Compiled May 17, 2017

ABSTRACT
There is extensive use of monochromatic lasers to select atoms with a narrow range of velocities in many atomic-physics experiments. For the commonplace situation of the inhomogeneous Doppler-broadened (Gaussian)linewidth exceeding the homogeneous (Lorentzian) natural linewidth by typically two orders of magnitude, a substantial narrowing of the velocity class of atoms interacting with the light can be achieved. However this is not always the case, and here we show that for a certain parameter regime there is essentially no selection—all of the atoms interact with the light in accordance with the velocity probability density. An explanation of this effect is provided, emphasizing the importance of the long tail of the constituent Lorentzian distribution in a Voigt profile.

KEYWORDS
Laser spectroscopy; velocity selection; Doppler broadening; Voigt profile

1. Introduction

Spectroscopic studies of absorption and emission lines in thermal atomic media were limited to the resolution of the Doppler width prior to the advent of the laser. A laser beam—taken to be a monochromatic light source in this paper—tuned exactly on to an atomic resonance will interact most strongly with atoms that have no component of velocity in the direction of propagation of the light. Strong interaction with moving atoms can be achieved by compensating for the Doppler effect by frequency detuning the light: as a consequence, the Doppler-broadened width of a spectral line is typically orders of magnitude broader than the natural linewidth for atomic media. With the availability of narrow-band radiation sources, it has become routine to generate sub-Doppler spectra with a resolution approaching the natural linewidth of the transition, typically by using pump-probe techniques (*1*, *2*). Here a narrow band of velocities, often centred on zero, is selected by e.g. arranging for the pump and probe beams to counter propagate. The location and width of the velocity class selected from the Doppler-broadened distribution provides the natural framework to explain many of these 'hole-burning' spectroscopic techniques that hinge on laser velocity-selective excitation (*3*, *4*).

CONTACT Ifan G. Hughes. Email: i.g.hughes@durham.ac.uk, ORCID http://orcid.org/0000-0001-6322-6435

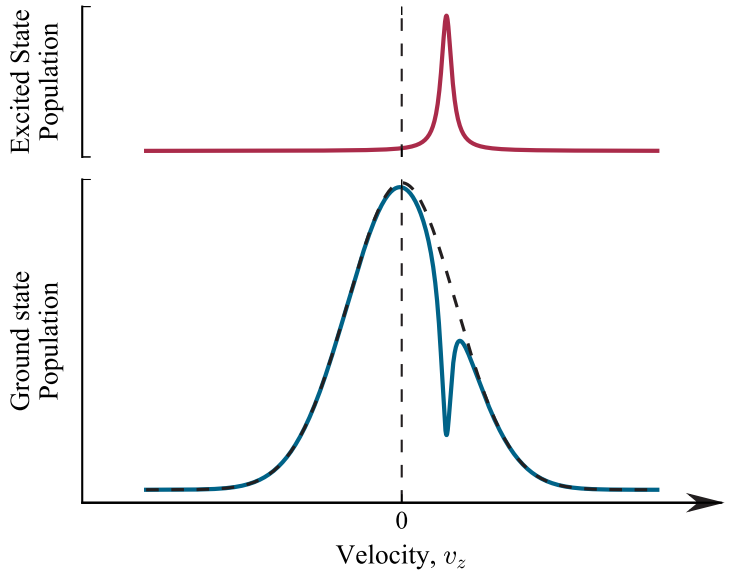

Figure 1. Principle of velocity-selective laser excitation. A laser with detuning Δ from resonance illuminates a medium of two-level atoms, with the detuning being smaller than the Doppler width. The velocity group that exhibits the strongest atom-light interaction is centred on a velocity component along the axis of the laser of $v_z = \Delta/k$, where k is the laser's wavevector. A narrow 'hole' is burned into the velocity distribution, and only atoms within a narrow range of velocity components are promoted to the excited state.

The principle of selecting a narrow velocity class from a broad distribution is shown schematically in Figure 1. We consider a simple two-level atom, with a resonant angular transition frequency ω_0 and a laser of angular frequency ω; the detuning, Δ, is defined as $\Delta = \omega - \omega_0$. The natural linewidth of the excited state is Γ. (Here, and throughout the paper, the width refers to the full width at half maximum—FWHM—for each distribution.) The atoms have a broad velocity distribution, characterized by a width u. For species used extensively in experiments, such as alkali-metal atoms, the Doppler width ku, with k the laser's wavenumber, is typically two orders of magnitude larger than the natural width, Γ. (For Na, K, Rb and Cs on the D2 transition the ratio of Doppler to Lorentzian widths, ku/Γ, is 133, 127, 84.2, and 71.5, respectively.) A traveling laser beam interacts only with a class of atoms that are centred on a certain velocity projection, v_z, onto the direction of propagation of the light. For a non-zero detuning, atoms in a velocity class centred on a finite value will absorb more of the light. The central velocity component and width of the class are governed by the relation

$$\bar{v}_z \pm \delta v_z/2 = (\Delta \pm \Gamma/2)/k. \tag{1}$$

As is evident from Figure 1 it is predominantly atoms within this velocity range that are selectively excited to the upper state (*2*). The one-to-one correspondence between atom velocity and detuning for maximum absorption lies at the heart of many techniques for laser cooling of atoms and molecules (*2*, *3*).

The Doppler-shifted absorption technique is used extensively for determining velocity distributions in atomic beams (*5*). For an atomic beam with a range of velocities along an axis, atoms in a narrow velocity class can be selected. This is achieved by appropriate choice of detuning and by having an oblique angle between the laser prop-

agation direction and the beam's axis. As text-book examples (*6*) Haroche *et al.* have used such a velocity-selected beam to demonstrate many fascinating physical phenomena, including: observing the progressive decoherence of the 'meter' in a quantum measurement (*7*); generation of Einstein-Podolsky-Rosen pairs of atoms (*8*); a quantum memory with a single photon in a cavity (*9*); and seeing a single photon without destroying it (*10*).

One of the first pump-probe techniques to be developed with sub-Doppler spectroscopic features was polarization spectroscopy (*11*). Nakayama provided a theoretical model where velocity selective optical pumping, and concomitant hole burning, feature prominently (*12*). Later, more involved models of polarization spectroscopy were developed, emphasizing the importance of a careful treatment of the effects of atomic velocity (*13–15*). Velocity-selective polarization spectroscopy remains an active topic in atomic (*16*) and molecular physics (*17*); the importance of Doppler averaging in calculating the medium's response in pump-probe laser spectroscopy is well known (*18*).

Thermal atomic vapours are being utilized in a wide range of applications, including: chip-scale atomic clocks (*19*) and magnetometers (*20*), microwave electric field detection (*21*), microwave magnetic field imaging (*22*, *23*), orbital angular momentum transfer (*24*), quantum memories (*25*), and measuring the number density of an optically thick medium (*26*). In addition to utilizing the resonant absorption properties of atomic media (dominated by the imaginary part of the atomic susceptibility), there is widespread interest in the off-resonance behaviour of the atom-light interaction exploiting the real component of the atomic susceptibility. Interesting physical phenomena, such as light-drag enhancement by a highly dispersive vapor, rely on the use of an optically dense medium far off resonance (*27*).

The rest of the paper is organized as follows: In Section 2 we derive the absorption coefficient for a medium of two-level atoms interrogated by a single laser beam, taking into account the velocity distribution. The breakdown of the one-to-one correspondence between detuning and central selected velocity emerges in Section 3. The paper culminates with a discussion of the implications of the results, and possible future extensions. Whereas all of the analysis presented here is for a medium composed of two-level atoms, the extension to multi-level systems is discussed in the final section.

2. The Doppler-broadened absorption profile

Here we shall revisit the calculation of the absorption coefficient of a Doppler-broadened transition, paying particular attention to the question of which velocity classes of atoms contribute to the absorption at a given laser detuning. The model system considered is identical to that depicted in Figure 1.

For a laser propagating through a medium of length ℓ the intensity at the output, I, is related to the input intensity, I_0, by the Beer-Lambert law (*28*)

$$I = I_0 \exp\left(-\alpha\ell\right) = I_0 \exp\left(-N\sigma\ell\right). \tag{2}$$

Here α is the absorption coefficient, N is the number density of atoms, and σ the cross section. We now consider the two distributions that need to be convolved to calculate the Doppler-broadened absorption profile.

2.1. *The homogeneous natural lineshape*

The lineshape for the absorption cross section for a stationary two-level atom takes the form of a Lorentzian as a function of detuning, given by (*28*)

$$\sigma(\Delta) = \sigma_0 \frac{\Gamma^2}{4\Delta^2 + \Gamma^2}, \tag{3}$$

where σ_0 is the peak absorption cross section, and Γ is the rate of spontaneous emission from the excited state. For a two-level atom with pure radiative broadening it can be shown (*3*) that $\sigma_0 = 3\lambda_0^2/2\pi$, where λ_0 is the resonant wavelength. For alkali-metal atoms it is possible to include dipole-dipole interactions that preserve the Lorentzian lineshape, with a number-density dependent width (*29*); however here we consider a dilute medium where the atoms are more likely to leave the laser beam before they collide with each other. Moreover it is possible to include power broadening (*30*), which also preserves the Lorentzian lineshape but with a broader width, but we shall restrict our attention to the weak-excitation regime.

2.2. *The inhomogeneous Doppler-broadened lineshape*

In a vapour or gas in thermal equilibrium, the atoms have a Maxwell-Boltzmann velocity distribution, with a Gaussian distribution of velocity components along any particular direction (*5*, *31*). The probability for atoms to have a z-component of velocity within the range v_z to $v_z + \mathrm{d}v_z$ is $f(v_z)\,\mathrm{d}v_z$, where

$$f(v_z) = \sqrt{\frac{m}{2\pi k_\mathrm{B} T}} \exp\left[-\frac{m v_z^2}{2 k_\mathrm{B} T}\right] = \frac{2}{u}\sqrt{\frac{\ln 2}{\pi}} \exp\left[-\frac{4 \ln 2 v_z^2}{u^2}\right]. \tag{4}$$

Here m is the mass of the atom; T is the temperature of the sample; k_B is Boltzmann's constant; and we introduced the FWHM of the velocity distribution, u, with (*28*) $u = 2\sqrt{2 \ln 2 k_\mathrm{B} T/m}$.

2.3. *The convolved lineshape*

We now calculate the absorption lineshape by taking into account both natural and Doppler broadening. For an atom with velocity component v_z along the direction of propagation of the laser beam the Doppler effect leads to a modification of the detuning of the laser frequency from resonance: $\Delta \to \Delta' = \Delta - k v_z$. Therefore the cross section becomes

$$\sigma(\Delta,\, v_z) = \sigma_0 \frac{\Gamma^2}{4(\Delta - k v_z)^2 + \Gamma^2}, \tag{5a}$$

$$\sigma(\Delta,\, v_z) = \frac{\sigma_0 \Gamma^2}{k^2 u^2} \frac{1}{4(\Delta/ku - v_z/u)^2 + \Gamma^2/k^2 u^2}, \tag{5b}$$

$$\sigma(\Delta,\, v_z) = \frac{\sigma_0 \Gamma^2}{k^2 u^2}\, L\left(\frac{v_z}{u}, \frac{\Delta}{ku}\right). \tag{5c}$$

Here the function L is the normalised Lorentzian lineshape that we shall find convenient later. To obtain the absorption coefficient of the medium we need to sum contributions from all the atomic velocity groups:

$$\alpha(\Delta) = \int_{-\infty}^{\infty} n(v_z)\,\sigma(\Delta,\, v_z)\,\mathrm{d}v_z, \tag{6}$$

where the number density of atoms having a z-component of velocity within the range v_z to $v_z + \mathrm{d}v_z$ is $n(v_z)\,\mathrm{d}v_z = Nf(v_z)\,\mathrm{d}v_z$.

Inserting the expressions from equations (4) and (5) into equation (6), we obtain

$$\alpha(\Delta) = \frac{N\sigma_0\Gamma^2}{2u}\sqrt{\frac{\ln 2}{\pi}}\int_{-\infty}^{\infty}\frac{\exp\left[-4\ln 2 v_z^2/u^2\right]}{(\Delta - kv_z)^2 + \Gamma^2/4}\,\mathrm{d}v_z, \tag{7a}$$

$$\alpha(\Delta) = \frac{2N\sigma_0\Gamma^2}{k^2u^2}\sqrt{\frac{\ln 2}{\pi}}\int_{-\infty}^{\infty} f\left(\frac{v_z}{u}\right) L\left(\frac{v_z}{u}, \frac{\Delta}{ku}\right)\mathrm{d}v_z/u. \tag{7b}$$

This integral is the convolution of the Gaussian and Lorentzian functions, known as the Voigt profile (*1*). Unfortunately, this integral cannot be evaluated analytically, and historically one had to rely on tabulated values of the Voigt function (*32*). Fortunately, efficient computer algorithms now exist for its evaluation, meaning that least-squares techniques (*33*) can be used to fit experimental spectra (*34*).

In the limit that the Lorentzian can be approximated as a delta-function the narrow distribution 'picks out' the broad distribution in the convolution integral, and the Voigt lineshape reverts to the Gaussian. For many atoms of interest the Gaussian is approximately two orders of magnitude wider than the Lorentzian; however, as we go on to show in the next Section, the approximation that the convolution of a broad Gaussian and a narrow Lorentzian can always be reduced to a Gaussian is not universally valid.

3. Velocity selection

Figure 2 presents the main results of this investigation. In each panel two functions are plotted: the dashed red line shows $f(v_z/u)$, the velocity distribution (left-hand axis); the continuous blue line shows the integrand from equation (7), i.e. the product of the velocity distribution and the displaced Lorentzian. The abscissa for all the plots is the scaled velocity v_z/u. The ratio of Doppler to Lorentzian widths, ku/Γ, is 20. Panel (a) shows the case for zero detuning. To an excellent approximation, the atoms contributing to the absorption coefficient at this detuning follow a Lorentzian distribution. For (b) a finite detuning of $\Delta = 0.5\,ku$ is depicted, and as expected from the conventional text book argument a narrow velocity distribution, approximately a Lorentzian, centred at a velocity $v_z/u = 0.5$, is selected. This trend does not continue, however, for larger detunings.

In (c) we have $\Delta = 1.5\,ku$ and it is evident that the velocity classes selected do not follow a Lorentzian distribution. There is a narrow Lorentzian, but accompanied by a significant contribution from atoms with smaller values of v_z. This distortion of

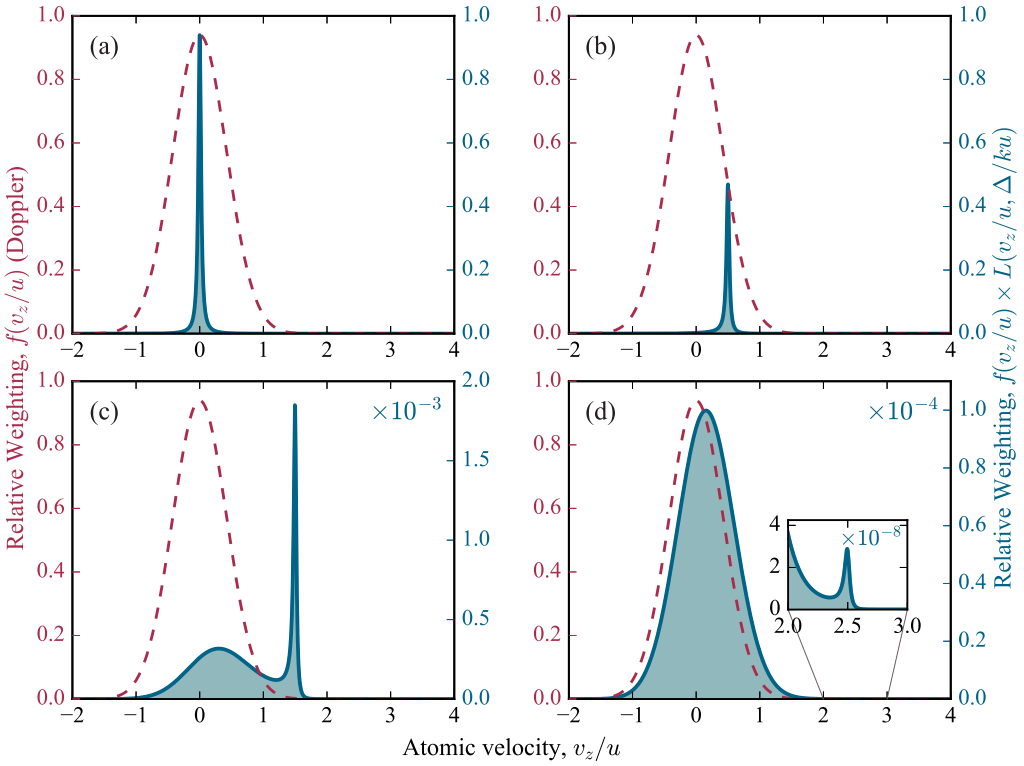

Figure 2. Each panel shows two functions as a function of the velocity component: the dashed red line shows $f\,(v_z/u)$, the Gaussian velocity distribution (left-hand axis); the continuous blue line shows the integrand from equation (7), i.e. the product of the velocity distribution and the displaced Lorentzian. The ratio of Doppler to Lorentzian widths, ku/Γ, is 20. Panel (a) shows the case for zero detuning, (b) has $\Delta = 0.5\,ku$, (c) $\Delta = 1.5\,ku$ and (d) $\Delta = 2.5\,ku$. To an excellent approximation, the atoms contributing to the absorption coefficient for the two smallest detuning follow a Lorentzian distribution, centred at a velocity $v_z = \Delta/k$. This trend does not continue, however, for larger detunings, as is evident from (c) and (d) where significantly broader velocity classes participate in the absorption. The area under the blue curve gives the absorption coefficient at each detuning.

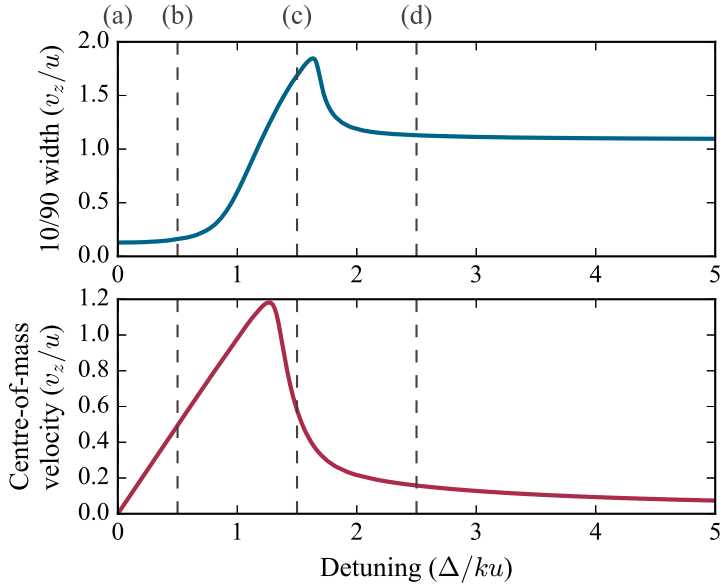

Figure 3. The upper panel shows the width, and the lower panel the centre-of-mass position of the velocity group selected as a function of the detuning scaled by the Doppler width. The lines denoted (a), (b), (c) and (d) correspond to the detunings chosen in the corresponding panels in Figure 2. For small detunings (i) the width is approximately equal to that of the Lorentzian, and (ii) there is a one-to-one correspondence between detuning and the central velocity; these results are in agreement with the prediction of Equation (1). For larger detunings these predictions become invalid: the width of the velocity class selected becomes approximately equal to that of the Gaussian, and the distribution is centred on zero velocity.

the velocity class selected is a consequence of two factors: (i) the rapid fall-off with frequency of the number of atoms with the appropriate velocity to be resonant, from equation (4); and (ii) the atom-light interaction is still non-zero far off resonance owing to the long-tailed nature of the Lorentzian distribution. For a detuning of $\Delta = 1.5\,ku$ there are far fewer atoms with the 'correct' velocity component to shift onto resonance compared to the zero-detuning case. Therefore the large number of atoms which are very far from resonance contribute as the $\sim 1/\Delta^2$ wing behaviour of the Lorentzian, from equation (3), decreases far slower than the Gaussian. In (d) a detuning of $\Delta = 2.5\,ku$ is depicted. Here the inset shows a minor contribution from a narrow peak at the expected value of $v_z = 2.5\,u$, however the distribution of the velocities selected here is far closer to the Gaussian.

Remarkably, for detunings of approximately two Doppler widths or larger atoms that are moving towards the laser (v_z negative), and consequently are Doppler shifted further from resonance, contribute nearly as strongly as the atoms with the 'correct' sign for their velocity component and hence Doppler shift. This is on account of the very large number of atoms that are many Lorentzian linewidths detuned contributing more significantly to the absorption than the exponentially smaller number of atoms with the velocity components to bring the laser onto resonance. Note also the significant change of scale for panels (c) and (d), reflecting the substantially lower value of the absorption coefficient for these detunings.

In the upper panel of Figure 3 we show the width of the velocity class selected, and in the lower panel the velocity centre-of-mass, both as a function of the detuning in units of the Doppler width. It is evident that the simple result of equation (1) for the width and centre of the selected velocity class has a limited domain of validity, failing completely for detunings exceeding one and a half Doppler widths.

The peculiar shape of the functions for large detunings renders the concept of FWHM to have limited utility, therefore we use the 10/90 width instead (defined as the difference in velocity component at which the cumulative integral of the distribution is 90% and the velocity at which the cumulative integral reaches 10%). For small detunings, the upper panel of figure 3 shows that the result is $0.14\,u$, which is consistent with the value of $2.87\,\Gamma$ for the Lorentzian, with $ku/\Gamma = 20$. Before the detuning reaches one Doppler width there is a dramatic increase in the width of the velocity distribution contributing to the absorption coefficient. For detunings exceeding two Doppler widths, the width of the selected velocity class is approximately equal to that of the Gaussian, as is expected from the distributions in figure 2 (c) and (d).

For detunings of up to approximately one Doppler width, the centre-of-mass of the selected (narrow) velocity class follows the linear prediction of equation (1) (with slope of 1 when the centre is scaled by the FWHM velocity, and the detuning by the FWHM Doppler width). However, before the detuning exceeds one and a half Doppler widths the centre-of-mass of the velocity class of the atoms contributing to the absorption rapidly decreases. The centering of the velocity class on zero velocity for large detunings reflects the form of the distributions, as is evident in figure 2 (c) and (d). Equation (1) predicts that a very fast packet of atoms would be selected by a detuning exceeding a few Doppler widths, yet counter-intuitively this is not the case; atoms with an extremely broad distribution of atomic velocities, essentially centred on zero velocity, interact with the laser.

4. Discussion and conclusion

One might argue that as the effects highlighted in the previous Section only become apparent at large detunings that they will never become important as there is so little absorption. This argument can be countered by taking into account two factors: (i) it is possible to have huge number densities, and consequently large off-resonance absorption, and (ii) the refractive index decreases less quickly as a function of detuning in the wing of the absorption profile. For thermal ensembles of alkali-metal atoms in particular, it is easy to increase the number density substantially by a modest increase in temperature (see Appendix A of (*34*)). Understanding the interplay between refractive index and absorption (*35*) is crucial for certain optical phenomena, for example the off-resonant (*36*) and slow-light Faraday effect (*37*), and in designing optical components based on thermal atomic vapours, such as compact optical isolators (*38*), Faraday filters (*39–41*), magneto-optical transmission filters (*42*), Faraday dichroic beam splitters (*43*) and electromagnetically induced polarization rotators (*44*). Recent work has highlighted the importance of the precise experimental characterization of the susceptibility of an atomic medium inside an optical cavity, accounting for both homogeneous and inhomogeneous broadening at high optical densities, for the design and operation of quantum light-matter interfaces, particularly in the context of quantum information processing (*45–47*).

Alkali-metal atoms do not have the simple two-level structure considered here, but it is possible to explain their Doppler-broadened spectra by summing the contributions of the numerous overlapping Voigt profiles (*48*, *49*). In multilevel systems it is possible for hyperfine pumping to occur, where atoms are excited resonantly by the laser on an open transition, and via spontaneous emission can be transferred into another angular momentum state in the ground term which is so far from resonance that the state can be considered 'dark'. The role of hyperfine pumping in multilevel systems was

previously highlighted (*50–52*), and the modification of the properties of the hole burned in the velocity distribution as compared to Figure 1 is crucial, especially in the context of achieving a sufficiently weak beam that does not perturb the medium (*53*). The emergence of experiments with an optical fiber suspended in warm alkali-metal vapour has highlighted the importance of understanding the effect of the atomic transit times on the atom-light interaction (*54*, *55*).

In this paper, we restricted our attention to the simplest possible case of two atomic levels, and one laser field. There is also a vast body of literature on three-level systems coupled by two laser fields, with particular emphasis on the phenomenon of electromagnetically induced transparency (EIT); see (*56*) and references therein. A careful consideration of the velocity classes involved in the atom-light interaction is important for a quantitative agreement between theory and experiment (*57*). Again, most atoms of interest do not have only three levels, which can complicate the analysis. Although it was recently demonstrated that with a sufficiently large magnetic field the otherwise overlapping Doppler profiles can be separated, allowing demonstration of textbook three-level atom phenomena (*58*, *59*). Often using a dressed-state picture for multi-level systems allows for a better understanding, and allows incorporation of light shifts and uncoupled absorption (*60*, *61*). In dense media when trying to optimise EIT the interplay between inhomogeneous broadening and the existence of several excited levels may lead to a vanishing transparency, and it was a careful consideration and shaping of the atomic velocity distribution which allowed a 5-fold enhancement of the signal (*62*).

In summary, a ubiquitous textbook result for the centre and width of the velocity class excited from a thermal distribution by a narrowband laser has been shown to have a restricted domain of validity. For detunings exceeding approximately one Doppler width, the exponential suppression of the number of resonant atoms in addition to the long-tailed nature of the Lorentzian dominate the Voigt absorption profile. As a consequence a far broader velocity class is selected, which is not centred at the velocity where the Doppler shift cancels the detuning, but rather at zero. Incorporating this effect into calculations is likely to lead to a better understanding and more quantitative agreement for various atom-light interaction schemes.

Acknowledgements

This work was supported by the EPSRC under Grant EP/L023024/1. The data presented in this paper are available for download from http://doi:10.15128/r2rv042t058.

The author wishes to thank Aidan Arnold and Lee Weller for illuminating discussions; James Keaveney for assistance with the figures; and James Keaveney and Renju Mathew for a careful reading of the manuscript.

On a personal note the author would like to pay tribute to the late Prof. Danny Segal, who provided great enthusiasm for the field of ion trapping and cooling and laser spectroscopy. The author discussed the topic of this paper with Danny at a Summer School in Wales, and will always value the encouragement and support that he received from him at various stages in his career. The author benefited from interactions with Danny in different supervisory and pastoral roles, duties he discharged with grace and humour.

References

(1) Corney, A. *Atomic and Laser Spectroscopy*; Oxford University Press: Oxford, UK, 1980.
(2) Letokhov, V. *Laser Control of Atoms and Molecules*; Oxford University Press: Oxford, UK, 2007.
(3) Foot, C. J. *Atomic Physics*; Oxford University Press: Oxford, UK, 2005.
(4) Nagourney, W. *Quantum Electronics for Atomic Physics and Telecommunications*; Oxford University Press, Oxford, UK, 2014.
(5) Scoles, G. *Atomic and Molecular Beam Methods: Volume 1*; Oxford University Press: Oxford, UK, 1998.
(6) Haroche, S; Raimond, J-M. *Exploring the Quantum*; Oxford University Press: Oxford, UK, 2006.
(7) Brune, M.; Hagley, E.; Dreyer, J.; Maitre, X.; Maali, A.; Wunderlich, C.; Raimond, J. M; Haroche, S. Observing the progressive decoherence of the 'meter' in a quantum measurement *Physical Review Letters* **1996**, *77*, 4887–4890.
(8) Hagley, E.; Maitre, X.; Nogues, G.; Wunderlich, C.; Brune, M.; Raimond, J. M.; Haroche, S. Generation of Einstein-Podolsky-Rosen pairs of atoms *Physical Review Letters* **1997**, *79*, 1–5.
(9) Maitre, X.; Hagley, E.; Nogues, G.; Wunderlich, C.; Goy, P,; Brune, M.; Raimond, J. M.; Haroche, S. Quantum memory with a single photon in a cavity *Physical Review Letters* **1997**, *79*, 769–772.
(10) Nogues, G.; Rauschenbeutel, A.; Osnaghi, S.; Brune, M.; Raimond, J.M.; Haroche, S. Seeing a single photon without destroying it *Nature* **1999**, *400*, 239–242.
(11) Wieman, C; Hansch, T. W. Doppler-free laser polarization spectroscopy *Physical Review Letters* **1976**, *36*, 1170–1173.
(12) Nakayama, S. Theoretical analysis of Rb and Cs D2 lines in Doppler-free spectroscopic techniques with optical pumping *Japanese Journal of Applied Physics Part 1* **1985**, *24*, 1–7.
(13) Pearman, C. P.; Adams, C. S.; Cox, S. G.; Griffin, P. F.; Smith, D. A.; Hughes, I. G. Polarization spectroscopy of a closed atomic transition: applications to laser frequency locking *Journal of Physics B: Atomic, Molecular and Optical Physics* **2002**, *35*, 5141–5151.
(14) Harris, M. L.; Adams, C. S.; Cornish, S. L.; McLeod, I. C.; Tarleton, E.; Hughes, I. G. Polarization spectroscopy in rubidium and cesium *Physical Review A* **2006**, *73*, 062509.
(15) Do, H. D.; Moon, G.; Noh, H. R. Polarization spectroscopy of rubidium atoms: Theory and experiment *Physical Review A* **2008**, *77*, 032513.
(16) Yu, H.; Kim, S. J.; Kim, J. B. Velocity Selective Polarization Spectroscopy for Modulation-Free Dispersion Signals at Detuned Frequencies *Journal of Spectroscopy* **2014**, *2014*, 541063.
(17) Kirkbride, J.; Dalton, A. R.; Ritchie, G. A. D. Polarization spectroscopy of a velocity-selected molecular sample *Optics Letters* **2014**, *39*, 2645–2648.
(18) Choi, G. W.; Noh, H. R. On the Doppler averaging of susceptibility in pump-probe laser spectroscopy *Optical Review* **2015**, *22*, 521–525.
(19) Knappe, S.; Shah, V.; Schwindt, P. D. D.; Hollberg, L.; Kitching, J.; Liew, L.; Moreland, J. A microfabricated atomic clock *Applied Physics Letters* **2004**, *85* 1460.
(20) Budker, D.; Romalis, M. Optical magnetometry *Nature Physics* **2007**, *3*, 227–234.
(21) Sedlacek, J. A.; Schwettmann, A.; Kübler, H.; Shaffer, J. P. Atom-Based Vector Microwave Electrometry Using Rubidium Rydberg Atoms in a Vapor Cell *Physical Review Letters* **2013**, *111*, 063001.
(22) Bohi, P.; Treutlein, P. Simple microwave field imaging technique using hot atomic vapor cells *Applied Physics Letters* **2012**, *101* 181107.
(23) Horsley, A,; Du, G. X.; Pellaton, M.; Affolderbach, C.; Mileti, G.; Treutlein, P. Imaging of relaxation times and microwave field strength in a microfabricated vapor cell *Physical Review A* **2013**, *88*, 063407.

(24) Walker, G.; Arnold, A. S,; Franke-Arnold, S. Trans-Spectral Orbital Angular Momentum Transfer via Four-Wave Mixing in Rb Vapor *Physical Review Letters* **2012**, *108*, 243601.
(25) Julsgaard, B.; Sherson, J.; Cirac, J. I.; Fiurášek, J.; Polzik, E. S. Experimental demonstration of quantum memory for light *Nature* **2004**, *432*, 482–486.
(26) Vliegen, E.; Kadlecek, S.; Anderson, L. W.; Walker, T. G.; Erickson, C. J. Happer, W. Faraday rotation density measurements of optically thick alkali metal vapors *Nuclear Instruments and Methods in Physics Research Section A* **2001**, *460*, 444–450.
(27) Safari, A.; De Leon, I.; Mirhosseini, M.; Magaña-Loaiza, O. S.; Boyd, R. W. Light-Drag Enhancement by a Highly Dispersive Rubidium Vapor *Physical Review Letters*, **2016**, *116*, 01360.
(28) Demtröder, W. *Laser Spectroscopy Basic Concepts and Instrumentation*; Springer, Berlin, 1996.
(29) Weller, L.; Bettles, R. J.; Siddons, P.; Adams, C. S.; Hughes, I. G. Absolute absorption on the rubidium D1 line including resonant dipole-dipole interactions *Journal of Physics B: Atomic, Molecular and Optical Physics* **2011**, *44*, 195006.
(30) Loudon, R. *The Quantum Theory of Light*; Oxford University Press: Oxford, UK, 2000.
(31) Ramsey, N. F. *Molecular Beams*; Oxford University Press: Oxford, UK, 1956.
(32) Thorne, A. P. *Spectrophysics*; Chapman and Hall: London, 1988.
(33) Hughes, I. G.; Hase, T. P. A. *Measurements And Their Uncertainties: A practical Guide to Modern Error Analysis*; Oxford University Press: Oxford, UK, 2010.
(34) Zentile, M. A.; Keaveney, J.; Weller, L.; Whiting, D. J.; Adams, C. S.; Hughes, I. G. ElecSus: A program to calculate the electric susceptibility of an atomic ensemble *Computer Physics Communications* **2015**, *189*, 162–174.
(35) Siddons, P.; Adams, C. S.; Hughes, I. G. Off-resonance absorption and dispersion in vapours of hot alkali-metal atoms. *Journal of Physics B: Atomic, Molecular and Optical Physics* **2009**, *42*, 175004.
(36) Kemp, S. L.; Hughes, I. G.; Cornish, S. L. An analytical model of off-resonant Faraday rotation in hot alkali metal vapours *Journal of Physics B: Atomic, Molecular and Optical Physics* **2011**, *44*, 235004.
(37) Siddons, P.; Bell, N. C.; Cai, Y.; Adams, C. S.; Hughes, I. G. A gigahertz-bandwidth atomic probe based on the slow-light Faraday effect *Nature Photonics* **2009**, *3*, 225–229.
(38) Weller, L.; Kleinbach, K. S.; Zentile, M. A.; Knappe, S.; Hughes, I. G.; Adams, C. S. Optical isolator using an atomic vapor in the hyperfine Paschen-Back regime *Optics Letters* **2012**, *37* 3405–3407.
(39) Yeh, P. Dispersive magnetooptic filters *Applied Optics* **1982**, *21*, 2069–2075.
(40) Zentile, M. A.; Whiting, D. J.; Keaveney, J.; Adams, C. S.; Hughes, I. G. Atomic Faraday filter with equivalent noise bandwidth less than 1 GHz *Optics Letters* **2015**, *40*, 2000–2003.
(41) Zentile, M. A.; Keaveney, J.; Mathew, R. S.; Whiting, D. J.; Adams, C. S.; Hughes, I. G. Optimization of atomic Faraday filters in the presence of homogeneous line broadening *Journal of Physics B: Atomic, Molecular and Optical Physics* **2015**, *48*, 185001.
(42) Rotondaro, M. D.; Zhdanov, B. V.; Knize, R. J. Generalized treatment of magneto-optical transmission filters *Journal of the Optical Society of America B* **2015**, *32*, 2507–2513.
(43) Abel, R. P.; Krohn, U.; Siddons, P.; Hughes, I. G.; Adams, C. S. Faraday dichroic beam splitter for Raman light using an isotopically pure alkali-metal-vapor cell *Optics Letters* **2009**, *34*, 3071–3073.
(44) Hombo, N.; Taniguchi, S.; Sugimura, S.; Fujita, K.; Mitsunaga, M. Electromagnetically induced polarization rotation in Na vapor *Journal of the Optical Society of America B* **2012**, *29*, 1717–1721.
(45) Kaczmarek, K. T.; Saunders, D. J.; Sprague, M. R.; Kolthammer, W. S.; Feizpour, A.; Ledingham, P. M.; Brecht, B.; Poem, E.; Walmsley, I. A.; Nunn, J. Ultrahigh and persistent optical depths of cesium in Kagomé-type hollow-core photonic crystal fibers *Optics Letters* **2015**, *40*, 5582–5585.
(46) Munns, J. H. D.; Qiu, C; Ledingham, P. M.; Walmsley, I. A.; Nunn, J.; Saunders, D. J.

In situ characterization of an optically thick atom-filled cavity *Physical Review A* **2016**, *93*, 013858.
(47) Heshami, K.; England, D. G.; Humphreys, P. C.; Bustard, P. J.; Acosta, V. M.; Nunn, J.; Sussman, B. J. Quantum memories: emerging applications and recent advances *Journal of Modern Optics* **2016**, *63*, 2005–2028.
(48) Siddons, P.; Adams, C. S.; Ge, C.; Hughes, I. G. Absolute absorption on rubidium D lines: comparison between theory and experiment *Journal of Physics B: Atomic, Molecular and Optical Physics* **2008**, *41*, 155004.
(49) Shin, S. R.; Noh, H. R. Doppler spectroscopy of arbitrarily polarized light in rubidium *Optics Communications*, **2011**, *284*, 1243–1246.
(50) Smith, D. A.; Hughes, I. G. The role of hyperfine pumping in multilevel systems exhibiting saturated absorption *American Journal of Physics* **2004**, *72*, 631–637.
(51) Himsworth, M.; Freegarde, T. Rubidium pump-probe spectroscopy: Comparison between ab initio theory and experiment *Physical Review A* **2010**, *81*, 023423.
(52) Noh, H. R.; Moon, G.; Jhe, W. Discrimination of the effects of saturation and optical pumping in velocity-dependent pump-probe spectroscopy of rubidium: A simple analytical study *Physical Review A* **2010**, *82*, 062517.
(53) Sherlock, B. E.; Hughes, I. G. How weak is a weak probe in laser spectroscopy? *American Journal of Physics* **2009**, *77*, 111–115.
(54) Jones, D. E.; Franson, D. E.; Pittman, T. B. Saturation of atomic transitions using subwavelength diameter tapered optical fibers in rubidium vapor *Journal of the Optical Society of America B*, **2014**, *31*, 1997–2001.
(55) Hickman, G. T.; Pittman, T. B.; Franson, J. D. Saturated absorption at nanowatt power levels using metastable xenon in a high-finesse optical cavity *Optics Express*, **2014**, *22*, 22882–22887.
(56) Marangos, J. P. Topical review electromagnetically induced transparency *Journal of Modern Optics* **1998**, *45*, 471–503.
(57) Gea-Banacloche, J.; Li, Y-Q.; Jin, S-Z.; Xiao, M. Electromagnetically induced transparency in ladder-type inhomogeneously broadened media: Theory and experiment *Physical Review A* **1995**, *51*, 576–584.
(58) Whiting, D. J.; Bimbard, E.; Keaveney, J.; Zentile, M. A.; Adams, C. S.; Hughes, I. G. Electromagnetically induced absorption in a nondegenerate three-level ladder system *Optics Letters* **2015**, *40*, 4289–4292.
(59) Whiting, D. J.; Keaveney, J.; Adams, C. S.; Hughes, I. G. Direct measurement of excited-state dipole matrix elements using electromagnetically induced transparency in the hyperfine Paschen-Back regime *Physical Review A* **2016**, *93*, 043854.
(60) de Echaniz, S. R.; Greentree, A. D.; Durrant, A. V.; Segal, D. M.; Marangos, J. P.; Vaccaro, J. A. Observations of a doubly driven V system probed to a fourth level in laser-cooled rubidium *Physical Review A* **2001**, *64*, 013812.
(61) Greentree, A. D.; Smith, T. B.; de Echaniz, S. R.; Durrant, A. V.; Marangos, J. P.; Segal, D. M.; Vaccaro, J. A. Resonant and off-resonant transients in electromagnetically induced transparency: Turn-on and turn-off dynamics *Physical Review A* **2002**, *65*, 053802.
(62) Scherman, M.; Mishina, O. S.; Lombardi, P.; Giacobino, E.; Laurat, J. Enhancing electromagnetically-induced transparency in a multilevel broadened medium *Optics Express* **2012**, *20*, 4346–4351.